

# Compound archery bow asymmetry in the vertical plane

Ihor Zanevskyy

Published online: 27 April 2012

© The Author(s) 2012. This article is published with open access at Springerlink.com

**Abstract** The aim of the research was to create a mechanical and mathematical model of a compound bow and analyse its work without any prior hypothesis about the symmetry of limb deflection. The method of the research was based on the methods of theoretical mechanics, applied and computer mathematics. A pair and shift mechanism with cams and levels was used as a basis of the mechanical and mathematical model of a compound bow. The difference between results of modelling and measurement was near 7 %, while the error due to digital image deformation was evaluated to be near 1 % which was considered as acceptable. The calculated results indicated noticeable differences from simulations using the constraint of symmetrical limb deformation. Comparison of symmetrical and asymmetrical simulations with experimental data revealed that the asymmetrical simulation gave a closer match to the measured values for cam angles; the simulated and measured cam angle asymmetry was much greater than any measurement errors. Realisation of a process of solving the problem using computer mathematical system MathCAD makes it possible for specialists of physical education and sports (coaches and sport archers), who do not have a mathematical background, to use the mechanical and mathematical model that was proposed in the research for a study and training process.

**Keywords** Archery · Compound bow · Mechanical and mathematical modelling

## List of symbols

$s_B$	Half-length of the string between cams
$h_U, h_L$	Riser lengths
$l$	Length of a limb
$\alpha_B$	Limb angle against a normal to the riser when a string is braced
$\alpha_0$	Angle of a free limb against a normal to the riser
$x_{NB}$	Clearance of a bow
$R, r$	Cam radii
$c_B$	Cable length between a cam and a limb when a string is braced
$F_{CB}$	Cable force when a string is braced
$F_{SB}$	String force when a string is braced
$k$	Stiffness of a limb
$\alpha_U, \alpha_L$	Angles of upper and lower limbs
$\beta_U, \beta_L$	Central angles of cams' sectors without a string
$s_U, s_L$	Distances along a string between cam and a nock point
$\gamma_U, \gamma_L$	Angles of the string incline
$y_N$	Transverse coordinate of the nock point
$x_N$	Longitudinal coordinate of the nock point
$\varphi$	Angles of revolution of cams
$c$	Cable length between a cam and a limb in the drawn situation
$c_B$	Cable length between a cam and a limb in the braced situation
$F_{SU}, F_{SL}$	String forces
$F_{CU}, F_{CL}$	Cable forces
$F_{Nx}, F_{Ny}$	Longitudinal and transverse components of the bow force
$F_N$	Bow force
$F_H$	Grip force
$G$	Weight of a bow

I. Zanevskyy (✉)  
Department of Physical and Health Education,  
Professor dr. hab. Casimir Pulaski Technical University,  
PR KWFIZ, ul. Malczewskiego 22, 26-600 Radom, Poland  
e-mail: i.zanevskyy@pr.radom.pl

$F_G$	Vertical component of the grip force
$\Delta$	Half part of the difference between the lengths of lower and upper branches of a string in the braced situation
$a$	Distance between the grip point and a straight line that connects axes of limbs and riser joints
$f$	Relative distance that defines a cam asymmetry

## 1 Introduction

The results in archery, like other sports of shooting, are strongly dependent on the quality of the sports weapon and its tuning. Experimental studies of traditional and recurved bows began at the start of their widespread use as a sport weapon. Mechanical and mathematical models of FITA (International Archery Federation) standard archery bow and a compound archery bow have been designed [1]. Because of differences in the mechanisms of the string and limb connection, there are different schemes of models. Modelling based on the scheme of the long bow has been developed much better than modelling of the compound bow. Investigations on the problems of compound archery bows have only been reported recently [8].

During the last five decades since their introduction, compound bows have become a popular sport weapon and now constitute the most popular kind of archery [2]. In comparison with other archery bows, the compound bow is able to store more energy and give higher accuracy in shooting. They are also more resistant to temperature and humidity changes due to the incorporation of string limbs in their design.

The first mechanical and mathematical model of the traditional English bow was proposed by Hickman [3] who studied static and dynamic behaviour of the bow. Klopsteg [4], using photo strobe method, described archery paradox. The issue is that an archery arrow has a flexible shaft that bends and buckles because of a compression force and a force impulse along its length occurs when a string slides from the fingers. Marlow [7] took into account elasticity of the string and calculated the energy fraction that transfers from limbs to an arrow. Mechanical and mathematical models of the archery paradox were elaborated by Pekalski [9] who explained lateral deflection of the arrow and bow rotation relatively vertical axis during their common motion. A model of recurved limbs was developed by Kooi [5, 6]. The author studied vibrations and stability in the vertical and transverse planes of the bow [10, 11]. The investigation has been done basing on the model of the bow in its main plane as an asymmetrical mechanical chain.

Scientific research of compound archery bow mechanics assuming symmetrical bending of upper and lower limbs was described by Park [8]. His basic mechanical and mathematical model of the compound bow needs to be developed. As a first step towards this model it is necessary to test a hypothesis about symmetrical bending of the limbs.

The aim of this research was to create a mechanical and mathematical model of a compound bow and analyse its work without of any prior hypothesis about the symmetry of limbs' deflection.

## 2 Braced bow situation

Upper and lower limbs of compound bows are identical and are braced symmetrically (Fig. 1). Considering a compound archery bow designed with a symmetrical twin cam and cable system a limb can be modelled with a solid shaft jointed to a handle using an Archimedean spring. Assuming constant spring stiffness the braced situation of the bow can be described by Eqs. (1)–(5):

$$2s_B = h_U + h_L + 2l \sin \alpha_B; \quad (1)$$

$$x_{NB} = l \cos \alpha_B + \rho; \quad (2)$$

$$2s_B = c_B; \quad (3)$$

$$F_{SB} \rho = F_{CB} r; \quad (4)$$

$$(F_{SB} + 2F_{CB}) l \cos \alpha_B = k(\alpha_0 - \alpha_B), \quad (5)$$

where  $\rho = \rho(\varphi)$  is a cam's radius with respect to a string, i.e. a distance from a cam's centre to the string (Fig. 2).

Equations (1) and (2) were derived using geometrical parameters of a bow kinematical chain. Equation (3) defines equal length of cable and string branches. As the angle between them is small, the cosine is taken to be equal to 1. The corresponding error for modern compound bows is around 0.1 % that is quite appropriate considering the accuracy of measuring bow parameters. Equations (4) and (5) represent cam equilibrium and limb equilibrium, respectively.

## 3 Drawn bow situation

A drawn situation of the bow (Fig. 3) is modelled using Eqs. (7)–(14):

$$h_U + l \sin \alpha_U + \rho \sin \beta_U = s_U \sin \gamma_U + y_N; \quad (6)$$

$$h_L + l \sin \alpha_L + \rho \sin \beta_L = s_L \sin \gamma_L - y_N; \quad (7)$$

$$x_N = l \cos \alpha_U + \rho \cos \beta_U + s_U \cos \gamma_U; \quad (8)$$

$$x_N = l \cos \alpha_L + \rho \cos \beta_L + s_L \cos \gamma_L; \quad (9)$$

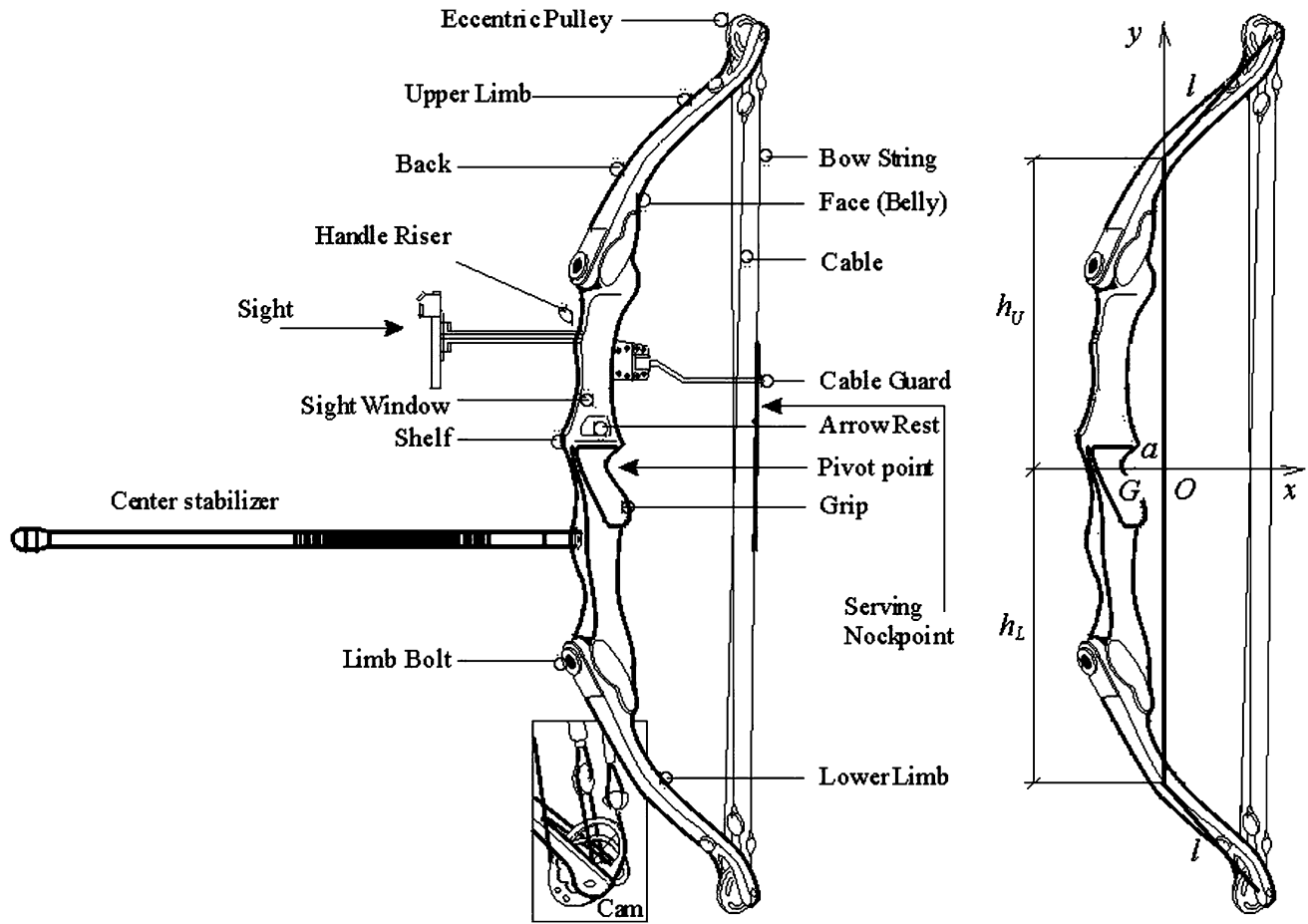


Fig. 1 Compound archery bow and bow scheme (<http://www.archery.org>)

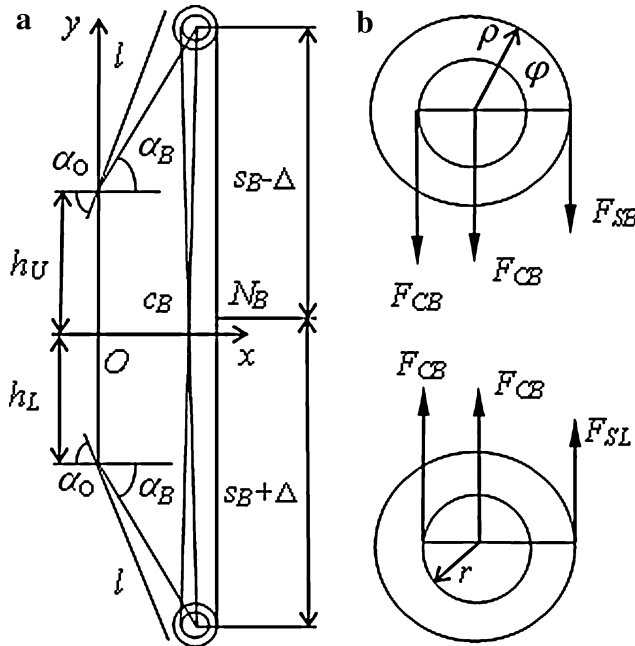


Fig. 2 Schematic images of a braced bow: **a** bow and **b** cams

$$c = h_U + h_L + l(\sin \alpha_U + \sin \alpha_L); \quad (10)$$

$$\beta_U + \gamma_U = \frac{\pi}{2}; \quad \beta_L + \gamma_L = \frac{\pi}{2}; \quad (11)$$

$$F_{SU}\rho = F_{CU}r; \quad F_{SL}\rho = F_{CL}r; \quad (12)$$

$$F_{Nx} = F_{SU} \cos \gamma_U + F_{SL} \cos \gamma_L; \quad (13)$$

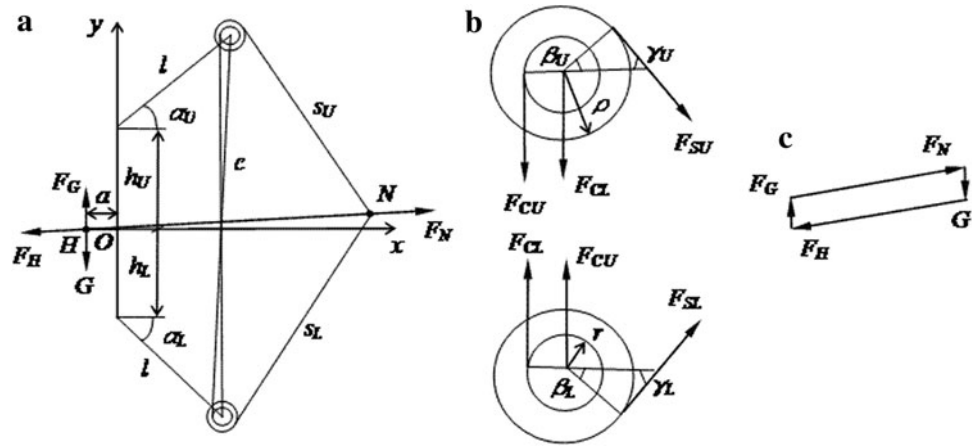
$$F_{Ny} = F_{SL} \sin \gamma_L - F_{SU} \sin \gamma_U;$$

$$\left[ \begin{array}{l} (F_{CU} + F_{CL}) \cos \alpha_U + \\ F_{SU} \sin \left( \frac{\pi}{2} - \alpha_U + \beta_U \right) \end{array} \right] l = k(\alpha_0 - \alpha_U); \quad (14)$$

$$\left[ \begin{array}{l} (F_{CU} + F_{CL}) \cos \alpha_L + \\ F_{SL} \sin \left( \frac{\pi}{2} - \alpha_L + \beta_L \right) \end{array} \right] l = k(\alpha_0 - \alpha_L).$$

Equations (6)–(9) describe the geometrical parameters of a bow kinematic chain. Equation (10) determines the cable length based on the assumption that it makes a very small angle with a riser. Equations (11) show the correlation between cam angles and string incline angles. Conditions of cams equilibrium are described in Eq. (12).

**Fig. 3** Schematic image of a drawn bow: **a** bow, **b** cams and **c** poly-angle of force vectors



Conditions of limbs equilibrium are described by Eq. (14). Longitudinal and transverse components of the draw force are presented in Eq. (13).

The geometrical parameters of a bow in the braced and drawn situations (see Figs. 2, 3) are related by Eqs. (15) and (16):

$$s_U = s_B - \Delta + \int_0^{\varphi+\beta_U} \rho d\vartheta; s_L = s_B + \Delta + \int_0^{\varphi+\beta_L} \rho d\vartheta; \quad (15)$$

$$c_B - c = r\varphi. \quad (16)$$

Equation (15) describe the correlation between the lengths of string branches and cam angles. Equation (16) describes the correlation between the lengths of cam branches and cam angles. Mechanical equilibrium of a bow is defined by Eq. (17).

$$\vec{F}_G = \vec{F}_N, \quad (17)$$

where  $F_N = \sqrt{F_{Nx}^2 + F_{Ny}^2}$  is a draw force. As the centre of gravity of the bow is situated near to the grip point, it can be assumed that the gravity force is balanced by the vertical component of a grip force:  $\vec{F}_G = \vec{G}$  (see Fig. 3c).

According to Eq. (17), the vector direction of a draw force can be represented as a straight line between the grip point and the nock point and written as:

$$\frac{F_{Ny}}{F_{Nx}} = \frac{y_N}{x_N + a}, \quad (18)$$

where  $a \equiv GO$  is a distance between the grip point and a straight line that connects axes of limbs and riser joints (see Figs. 1 and 3c).

#### 4 Example

Using an experimental compound archery bow (No. 028815P) with the parameters in Table 1, a cosine wave

**Table 1** Initial parameters

No	Designation	Dimension	Data
1	$l$	m	0.177
2	$h_U$	m	0.338
3	$h_L$	m	0.338
4	$R$	m	0.033
5	$r$	m	0.020
6	$k$	Nm	114.0
7	$\alpha_0$	rad	0.977
8	$\alpha_B$	rad	0.421
9	$\Delta$	m	0.040
10	$a$	m	-0.016
11	$x_N$	m	0.738
12	$f$	1	1.3

(Eq. (19)) was used to model the displacement in the transverse direction:

$$\rho(\theta) = R(f + \cos \theta). \quad (19)$$

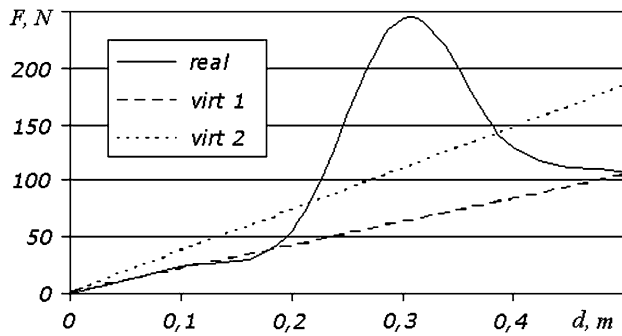
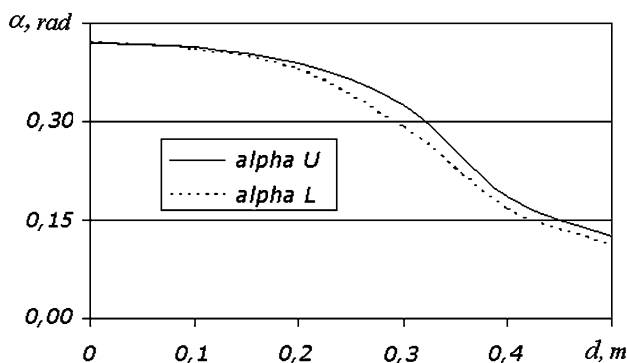
where  $R$  is a distinctive dimension of a cam. According to Eq. (19) the maximum radius of the cam on loading equals:  $\rho_{\max} = R(f + 1)$  and the minimum— $\rho_{\min} = R(f - 1)$ .

No analytical solution exists for the non-linear Eqs. (1)–(19), and so these were solved using a modified Newton–Raphson method for a system of algebraic equations using the MathCAD “Find” computer package. The computer programme used is presented in “Appendix”. Results of these calculations are presented in Table 2.

Graphs of a draw force of the real compound bow and corresponding virtual recurved bows with an equal force and equal energy are shown in Fig. 4. The amount of potential energy accumulated in the compound bow is 75 % greater than in the virtual recurved bow (virt 1) that has the same force. The draw force of the compound bow in the aiming situation is 2.3 times smaller than in the

**Table 2** Results of calculations

No	Designation	Dimension	Asymmetry model data	Symmetry model data	Difference, %
1	$\alpha_U$	rad	0.124	0.117	−5.6
2	$\alpha_L$	rad	0.110	0.117	6.4
3	$\beta_U$	rad	0.968	0.967	−0.1
4	$\beta_L$	rad	0.819	0.820	0.1
5	$\gamma_U$	rad	0.603	0.603	0.0
6	$\gamma_L$	rad	0.751	0.751	0.0
7	$s_U$	m	0.631	0.631	0.0
8	$s_L$	m	0.699	0.699	0.0
9	$c$	m	0.717	0.717	0.0
10	$c_B$	m	0.821	0.821	0.0
11	$\varphi$	rad	5.159	5.159	0.0
12	$x_{NB}$	m	0.238	0.238	0.0
13	$s_B$	m	0.410	0.410	0.0
14	$F_U$	N	66.0	66.1	0.2
15	$F_L$	N	68.6	68.5	−0.1
16	$F_x$	N	104.5	104.5	0.0
17	$F_y$	N	9.4	9.2	−2.1
18	$F_{CU}$	N	251.7	252.2	0.2
19	$F_{CL}$	N	257.9	257.4	−0.2
20	$y_N$	m	0.065	0.064	−1.5

**Fig. 4** Draw force of a compound bow (*real*) and correspondent virtual recurved bows with an equal force (*virt 1*) and equal energy (*virt 2*)**Fig. 5** Angles of upper (*U*) and lower (*L*) limbs

virtual recurved bow (*virt 2*) under the same amount of potential energy.

Figure 5 shows the predicted values for the limb angles as a function of draw displacement ( $d = x_N - x_{NB}$ ). In the braced situation the angles are equal. In the full drawn situation a difference between upper and lower limbs of 0.014 rad or  $\delta\alpha = 12.0\%$  is predicted compared to a common average value of them from a first estimate using a symmetrical approach, where:

$$\delta\alpha = \frac{200(\alpha_U - \alpha_L)}{\alpha_U + \alpha_L} \% \quad (20)$$

This difference is essential because it is many times greater than measurement errors of bow parameters ( $<1\%$ ).

The use of MathCAD in solving this system of equations makes it possible for specialists of physical education and sports (coaches and sport archers), who do not have a strong mathematical background, to use the mechanical and mathematical model developed in this programme for study and training purposes.

The model requires 12 initial real compound bow parameters, whilst predicting a further 20 to give 32 bow parameters in total.

In contrast to other approaches (e.g., Park [8]) there is no a priori hypothesis about symmetrical deflection of upper and lower limbs. Relaxation of this condition

results in a predicted asymmetry in the limb deflections of about 12 %. This value is 1–2 orders of magnitude greater than errors in measurements of the main bow parameters.

Considering the “symmetrical” model, the equation governing this model is below:

$$\alpha_U = \alpha_L. \quad (21)$$

Inclusion of Eq. (21) in the system of Eqs. (1)–(16), (18), and (19) can be achieved by artificial modification of the limbs stiffness. As the deflection of the lower limb is predicted to be smaller (see Fig. 4), its stiffness needs to be decreased and that of the upper limb increased. As a result Eqs. (14) becomes:

$$\begin{cases} (F_{CU} + F_{CL}) \cos \alpha_U \\ + F_{SU} \sin\left(\frac{\pi}{2} - \alpha_U + \beta_U\right) \end{cases} l = (k - \kappa)(\alpha_0 - \alpha_U); \quad (22)$$

$$\begin{cases} (F_{CU} + F_{CL}) \cos \alpha_L \\ + F_{SL} \sin\left(\frac{\pi}{2} - \alpha_L + \beta_L\right) \end{cases} l = (k + \kappa)(\alpha_0 - \alpha_L),$$

where  $\kappa$  is a value of limb stiffness correction. So, the system of Eqs. (1)–(13), (15), (16), (18), (19), (21), and (22) are a mathematical model of the bow for a symmetrical limb deflection condition. Results of the simulations using both symmetrical and asymmetrical conditions for a fully drawn situation ( $x_N = 0.738$  m) are presented in Table 2. The value of stiffness correction,  $\kappa$ , used in these simulations was 0.89 Nm (Fig. 6).

The relative differences between these simulations were greatest for the limb angles ( $>5$  % and in the case of the lower limb it is greater). The differences in transverse component of the draw force ( $-2.1$  %) and transverse displacement of a nocking point ( $-1.5$  %) were significant too. The differences regarding cam and string forces ( $0.1$ – $0.2$  %) are near the errors of measurements of bow parameters and so not noticeable. Any other differences which describe longitudinal parameters were negligibly small (near  $0.05$  %) and this is reasonable because “symmetrical” hypothesis deals with transverse parameters.

#### 4.1 Experimental verification of the model

An experimental archery bow (No. 028815P) was hung at the grip point  $G$  and loaded gravitationally with  $W$ -load at the nock point  $N$  (Fig. 7). A photographic image of the drawn bow was captured using a digital camera which was situated with its optical axis normal to the vertical plane of the bow.

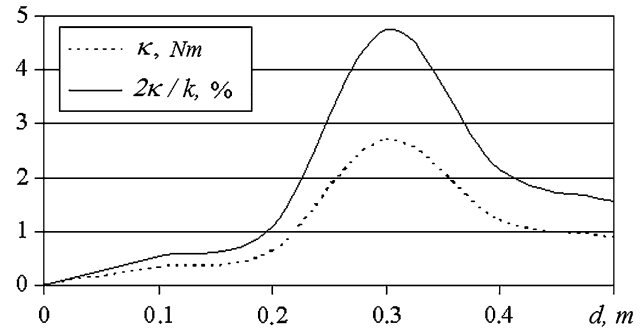


Fig. 6 A value of limb stiffness correction

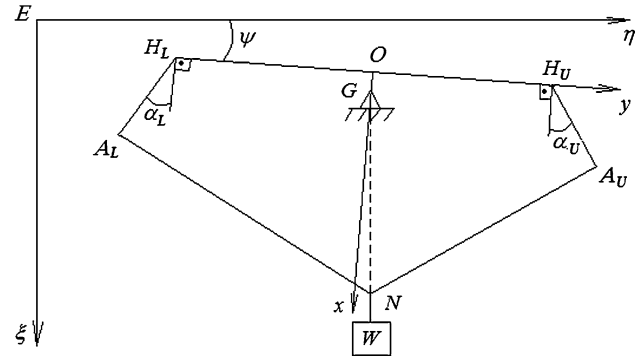


Fig. 7 Schematic diagram of the gravitationally loaded experimental bow

Table 3 Bow points coordinates

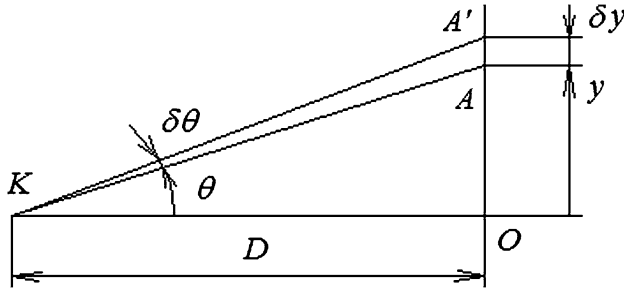
Point	Coordinates, pixel	
	$\xi$	$\eta$
O	115	646
G	134	643
A <sub>U</sub>	388	1,096
A <sub>L</sub>	303	157
H <sub>U</sub>	154	1,087
H <sub>L</sub>	76	203
N	1,089	645

The digital image was situated with its vertical line  $GN$  in parallel to a side border of MS Paint worktable. A scale of the bow image was calculated using a ruler on the bow riser ( $\mu = 0.761$  mm/pixel). Coordinates of the calm axes ( $A_U$ ,  $A_L$ ), the handle grip ( $G$ ) and the limbs virtual joint points ( $H_U$ ,  $H_L$ ), the nock point ( $N$ ), and the origin ( $O$ ) of Oxy coordinate system were measured in pixels (Table 3).

Geometrical parameters were compared with results of modelling (see Table 2) using the equations below:

**Table 4** Comparison of measurement and simulation

Parameter	Dimension	Measurement	Simulation	Difference, %
ON	mm	741	741	0
$tg\psi$	1	0.088	0.090	2.3
$\alpha_U$	rad	0.125	0.124	-0.8
$\alpha_L$	rad	0.106	0.110	3.8
W	N	98.1	104.9	7.0

**Fig. 8** Schematic diagram of digital image errors

$$\begin{aligned}
 NO &= \mu \sqrt{(\xi_N - \xi_O)^2 + (\eta_N - \eta_O)^2} = 741 \text{ mm}; \\
 NO &= \sqrt{x_N^2 + y_N^2} = 741 \text{ mm}; \\
 tg\psi &= \frac{\xi_{HU} - \xi_{HL}}{\eta_{HU} - \eta_{HL}} = 0.088; \\
 tg\psi &= \frac{y_N}{x_N + a} = 0.090 \text{ (see Eq.18);} \\
 \cos(\angle A_U H_U H_L) &= \frac{l^2 + (h_U + h_L)^2 - (H_L A_U)^2}{2l(h_U + h_L)} \\
 &= -0.1249; \angle A_U H_U H_L = 1.696; \\
 \alpha_U &= \angle A_U H_U H_L - \frac{\pi}{2} = 0.125; \\
 \cos(\angle A_L H_L H_U) &= \frac{l^2 + (h_U + h_L)^2 - (H_U A_L)^2}{2l(h_U + h_L)} \\
 &= -0.1063; \angle A_L H_L H_U = 1.677; \\
 \alpha_L &= \angle A_L H_L H_U - \frac{\pi}{2} = 0.106. \quad (23)
 \end{aligned}$$

Comparative results of measurement and simulation are presented in Table 4. The error associated with digital imaging of the limbs' deflection was also evaluated (Fig. 8):  $D$  is the distance from a camera to the vertical plane of symmetry of the bow;  $AA''$  is a small displacement in the plane  $\left(\frac{\delta y}{D} \ll 1\right)$ . Using a small angle approximation ( $\delta\theta \ll 1$ ), the measurement error was estimated. For e.g., corresponding equations along Oy axis are as below:

$$y = Dtg\theta; \delta y_{y=0} \approx D\delta\theta; \delta y = Dtg(\theta + \delta\theta) - y. \quad (24)$$

Taking into account the equality  $tg(\theta + \delta\theta) \approx \frac{tg\theta + \delta\theta}{1 - tg\theta \times \delta\theta}$ , gives:

$$\delta y \approx \frac{1 + tg^2\theta}{1 - tg\theta \times \delta\theta} D\delta\theta; \quad \frac{\delta y}{\delta y_{y=0}} \approx \frac{1 + tg^2\theta}{1 - tg\theta \times \delta\theta}. \quad (25)$$

The relative error in a digital image is  $\lim_{\delta\theta \rightarrow 0} \left( \frac{\delta y}{\delta y_{y=0}} \right) = 1 + tg^2\theta$ .

The character dimensions of the bow in the main plane are  $y = 0.4$  m,  $D = 4.0$  m, giving a value of 1 %. Given the level of error, then the differences between symmetrical and asymmetrical simulations (see Table 2) for cam angles are the most notable differences. Comparing the cam angle simulations,  $\alpha_U$  for the asymmetric simulation gives a much closer representation ( $-0.001$  rad) than the symmetric simulation ( $-0.008$  rad). The agreement of  $\alpha_L$  is less good, but is still closer (0.004 rad) for the asymmetric simulation than for the symmetric one (0.011 rad).

Although validation has been carried out for just one specific example to date and requires generalisation, the relaxation of symmetric cam angles appears to give greater accuracy in deflection simulation.

## 5 Conclusions

A mathematical model of the deformation of a compound bow has been formulated based on 12 input parameters from which a further 20 parameters are predicted.

The model relaxes the condition for symmetry between the cam angles and predicts a 12 % difference in the deflections of the two limbs.

The difference between results of simulation and measurement was up to 7 % while the error in digital imaging of deformation was around 1 %. Compared with a simulation involving symmetry many parameters were not significantly different. The cam angles were, however, different and the values from the asymmetric simulation were much closer than those from a symmetric simulation. Simulation of  $\alpha_U$  was much more accurate than that of  $\alpha_L$ .

**Acknowledgments** The research was partly supported by Polish Ministry of Science and Higher Education, Research Grant No 2814/58/P. The author thanks Anonymous Referee for fruitful remarks and English language corrections.

**Open Access** This article is distributed under the terms of the Creative Commons Attribution License which permits any use, distribution, and reproduction in any medium, provided the original author(s) and the source are credited.

## Appendix

MathCAD computer program.



$$\begin{aligned}
 l &= .177 & hu &= .338 & hL &= .338 & \alpha 0 &= .977384 & R &= .1 & r &= .02 & \Delta &= .04 & a &= -.016396 & d &= .5 \\
 \alpha u &:= \frac{\pi}{6} & \beta u &:= \frac{\pi}{4} & \gamma u &:= \frac{\pi}{4} & \phi u &:= \pi & \phi L &:= \pi & \alpha B &= .420656 & f &:= 1.3 & x &:= 1 \cdot \cos(\alpha B) + R \cdot \frac{(1+f)}{3} + d \\
 c &:= .4 & cB &:= .5 & SB &:= .5 & xB &:= .17 & Su &:= .6 & SL &:= .6 & y &:= 0 & k &= 114 \\
 \alpha L &:= \frac{\pi}{6} & \beta L &:= \frac{\pi}{4} & \gamma L &:= \frac{\pi}{4} & Fu &:= 100 & FL &:= 100 & Fcu &:= 100 & FcL &:= 100 & Fx &:= 200 & Fy &:= 0 & p &:= 3
 \end{aligned}$$

Given

$$\begin{aligned}
 hu + 1 \cdot \sin(\alpha u) + R \cdot \sin(\beta u) \cdot \frac{(\cos(\phi u + \beta u) + f)}{p} &= Su \cdot \sin(\gamma u) + y & \phi u &= \phi L & 2 \cdot SB &= cB \\
 hL + 1 \cdot \sin(\alpha L) + R \cdot \sin(\beta L) \cdot \frac{(\cos(\phi L + \beta L) + f)}{p} &= SL \cdot \sin(\gamma L) - y & c &= hu + hL + 1 \cdot (\sin(\alpha u) + \sin(\alpha L)) \\
 x = 1 \cdot \cos(\alpha u) + R \cdot \cos(\beta u) \cdot \frac{(\cos(\phi u + \beta u) + f)}{p} + Su \cdot \cos(\gamma u) & & \beta u + \gamma u &= \frac{\pi}{2} & \beta L + \gamma L &= \frac{\pi}{2} \\
 x = 1 \cdot \cos(\alpha L) + R \cdot \cos(\beta L) \cdot \frac{(\cos(\phi L + \beta L) + f)}{p} + SL \cdot \cos(\gamma L) & & xB &= 1 \cdot \cos(\alpha B) + R \cdot \frac{(1+f)}{3} \\
 Su = SB - \Delta + R \cdot \frac{[\sin(\phi u + \beta u) + f \cdot (\phi u + \beta u)]}{p} & & hu + hL + 2 \cdot 1 \cdot \sin(\alpha B) &= 2 \cdot SB \\
 SL = SB + \Delta + R \cdot \frac{[\sin(\phi L + \beta L) + f \cdot (\phi L + \beta L)]}{p} & & Fu \cdot R \cdot \frac{(\cos(\phi u + \beta u) + f)}{p} &= Fcu \cdot r \\
 Fy = -\sin(\gamma u) \cdot Fu + \sin(\gamma L) \cdot FL & & FL \cdot R \cdot \frac{(\cos(\phi L + \beta L) + f)}{p} &= FcL \cdot r \\
 Fx = \cos(\gamma u) \cdot Fu + \cos(\gamma L) \cdot FL & & cB - c &= r \cdot \phi u \\
 (Fcu + FcL) \cdot 1 \cdot \cos(\alpha u) + Fu \cdot 1 \cdot \sin\left(\beta u - \alpha u + \frac{\pi}{2}\right) &= k \cdot (\alpha 0 - \alpha u) & k &= 114 \\
 (Fcu + FcL) \cdot 1 \cdot \cos(\alpha L) + FL \cdot 1 \cdot \sin\left(\beta L - \alpha L + \frac{\pi}{2}\right) &= k \cdot (\alpha 0 - \alpha L) & x &= 0.738236
 \end{aligned}$$

$$Find(\alpha u, \alpha L, \beta u, \beta L, \gamma u, \gamma L, Su, SL, c, cB, \phi u, \phi L, xB, SB, Fu, FL, Fx, Fy, Fcu, FcL, y) =$$

	0	▲
0	0.124178	
1	0.110136	
2	0.967725	
3	0.819362	
4	0.603072	
5	0.751434	
6	0.630583	
7	0.699344	
8	0.717378	
9	0.820559	
10	5.159077	
11	5.159077	
12	0.238236	
13	0.41028	
14	66.009858	
15	68.644735	
16	104.524961	
17	9.423768	
18	251.695248	
19	257.86658	
20	0.06508	



## References

1. Compound Bow (2008) <http://www.archery.org>. Accessed 19 Apr 2012
2. Flewett WE (2007) The compound bow: twenty-five years after Allen's patent. <http://sagittarius.student.utwente.nl/artikel/compound>. Accessed 19 Apr 2012
3. Hickman CN (1937) Dynamics of a bow and arrow. *J Appl Phys* 8:404–409
4. Klopsteg PE (1943) Physics of bows and arrows. *Am J Phys* 11:175–192
5. Kooi BW (1981) On the mechanics of the bow and arrow. *J Eng Math* 15:119–145
6. Kooi BW (1991) On the mechanics of the modern working recurve bow. *Comput Mech* 8:291–304
7. Marlow WC (1981) Bow and arrow dynamics. *Am J Phys* 49:320–333
8. Park JL (2009) A compound archery bow dynamic model, suggesting modifications to improve accuracy. *Proc Inst Mech Eng Part P J Sports Eng Technol* 223(4):139–150
9. Pekalski R (1990) Experimental and theoretical research in archery. *J Sports Sci* 8:259–279
10. Zanevskyy I (2001) Lateral deflection of archery arrows. *Sports Eng* 4:23–42
11. Zanevskyy I (2006) Bow tuning in the vertical plane. *Sports Eng* 9:77–86